Radiochim. Acta **89**, 215–222 (2001)

Dosimetry related to SPECT and PET applications

By H. Herzog*

Institute of Medicine, Forschungszentrum Jülich GmbH, D-52425 Jülich, Germany

(Received December 10, 1999; accepted in revised form August 18, 2000)

Dosimetry / Radiation dose / Biodistribution / MIRD / Single photon emission computerized tomography / Positron emission tomography

Summary. Nuclear medicine methods permit the *in vivo* measurement of physiological and metabolic functions. For this purpose metabolically active molecules are labelled with radionuclides. After the injection, these radiopharmaceuticals can be detected from outside the body with appropriate detectors such as conventional gamma cameras, single photon emission computerized tomographs (SPECT), or positron emission tomographs (PET). As with any application of ionizing radiation the benefits of nuclear medicine (the diagnosis and treatment of disease) must be balanced against the risks of the procedures. Risks in nuclear medicine are evaluated through dosimetry, the calculation of the radiation dose estimates, in which the energy deposited by the radiation in human tissues is quantitated. The first step of dosimetry is the determination of the biodistribution, i.e. the spatial and temporal distribution of the radiopharmaceutical within the body. When a new radiopharmaceutical is introduced such data are first derived from *ex vivo* experiments in animals. Further evaluations of the biokinetics and dosimetry are carried out via quantitative measurements in humans using the nuclear medicine imaging equipment, applying whole-body planar and tomographic methods. Based on the knowledge of the biodistribution and using the framework introduced by the MIRD committee as well as by the ICRP, the radiation dose to single organs and to the total body can be calculated. The purpose of this paper is to review methods for measuring radiopharmaceutical biodistributions in humans and for calculating the appropriate radiation dose quantities.

Introduction

Nuclear medicine provides diagnostic procedures which allow the investigation of physiological and metabolic functions within the human body. For this purpose indicator substances are administered to the patient by intravenous injection, inhalation, or ingestion. The indicator substances are labelled with radionuclides so that their distribution can be determined by measuring the emitted radiation with appropriate radiation-sensitive instruments. The measured data are assembled into images such as planar scintigrams or tomographic images which are examined to obtain the medical diagnosis. Only part of the activity emitted from the radionuclides reaches the radiation detectors whereas the rest is absorbed within the body. Radiation absorbed in the body causes ionisation and excitation of atoms within the cells of the body, possibly leading to cellular damage. If unrepaired, this damage may lead to short term or long term negative effects in the organism. The total energy deposited per unit mass, called the absorbed dose, is generally accepted to be proportional to these risks, and thus an appropriate quantity for study of the possible effects of ionising radiation. In order to estimate the absorbed dose the biodistribution, i.e. the spatial and temporal quantitative distribution of the administered radiopharmaceutical must be determined. For this purpose, diagnostic instruments can be utilised directly within or in addition to the diagnostic examination. If this is not possible, biodistribution data must be derived from appropriate animal models. Based on the biodistribution, the dose to specific organs or to the whole-body is determined by relating the radioactivity to the radiation energy deposited throughout the body. The purpose of this paper is to review methods for determining the biodistribution of radiopharmaceuticals and the radiation dose in nuclear medicine, especially in its tomographic applications SPECT and PET, and to describe the framework for calculating dose estimates for single organs and the whole-body from these biodistribution data. This framework follows the recommendations of the MIRD (Medical Internal Radiation Dose) committee as well as those of the ICRP (International Commission of Radiation Protection).

*E-mail: h.herzog@fz-juelich.de

Biodistribution measurement of single photon emitters

The first step to estimate the radiation dose related to a newly developed radiopharmaceutical is to get knowledge about the biodistribution. Because radiopharmaceuticals are designed to image specific organs, quantitative uptake values for these organs are known from previous pharmacokinetic research. During the development of a radiopharmaceutical it is of general interest to know the uptake also of organs other than the organ of interest. The necessary measurements are done commonly in rodents, especially mice and rats. The percent of the injected activity found in individual organs is interpreted, usually through some extrapolation method, to imply the biodistribution in humans. An example of data obtained in such animal studies is given in Table 1 (taken from [1]).

Although biodistribution data obtained in animals are very important for the introduction of a radiopharmaceutical

Table 1. Biodistribution of ^{123}I-α-O-methyltyrosine in mouse organs in which significant activities were found (Schmidt *et al.* [1]). (Units are (%) injected activity, decay-corrected.)

Time (min)	Brain	Pancreas	Liver	Kidneys	Heart	Thyroid.
2.00	0.85	4.85	8.49	21.69	0.87	0.03
5.00	1.27	7.53	10.28	36.63	1.18	0.05
10.00	2.42	14.49	13.51	63.78	1.67	0.07
20.00	1.85	6.87	9.25	34.37	1.00	0.06
40.00	0.73	2.72	3.76	15.52	0.40	0.03
60.00	0.63	2.40	3.17	16.62	0.43	0.01
100.00	0.56	2.70	2.58	10.87	0.27	0.01

one has to take into account that there may be considerable differences to the human biodistribution. Therefore, the animal data have to be validated by quantitative measurements of biodistribution in humans. Commercial radiopharmaceuticals are practically exclusively developed for planar scintigraphy and SPECT. Clinical SPECT is usually applied as a qualitative imaging procedure. It is very rarely used for quantitative measurements, which will not be discussed here. The general method to obtain the biodistribution of single photon emitting activity is conjugate whole-body imaging, which combines anterior and posterior whole-body projections and which were already used before the introduction of SPECT [2, 3]. This kind of scanning can conveniently be performed by using double-headed SPECT cameras with opposite gamma camera detectors and a whole-body scanning capability (Fig. 1). The count rate of anterior (N_a) and posterior (N_p) whole-body projections are combined pixelwise by calculating the geometric mean (GM) of opposite pixels:

$$N_{GM} = (N_a N_p)^{1/2} \tag{1}$$

Equation (2) relates the geometric mean found at a specific image pixel i to the activity A_i within a tube under this pixel:

$$A_i = G(N_{GM})_i \, e^{(\mu/2)L_i} \frac{\mu d_i/2}{\sinh(\mu d_i/2)} \tag{2}$$

with

G:	Constant of measurement device involving efficiency etc,
N_a, N_p:	Count rate at pixel i in anterior or posterior view,
μ:	Absorption coefficient at pixel i, $L = l_1 + l_2$
L_i:	Body thickness at pixel i,
d_i:	Organ thickness at pixel i.

In conventional planar scintigraphy, the unknown depth of an organ is the decisive reason why scintigrams cannot be evaluated quantitatively, i.e. they do not yield calibrated values of radioactivity (kBq or nCi). Looking at a planar projection it is not possible to distinguish whether a decreased low count rate is caused by a low activity within the organ or by the organ depth, as much of the radiation emitted from this source is absorbed by the overlaying tissue. Using the geometric mean method the resulting data become independent of the depth of a single organ within the body as apparent from (2).

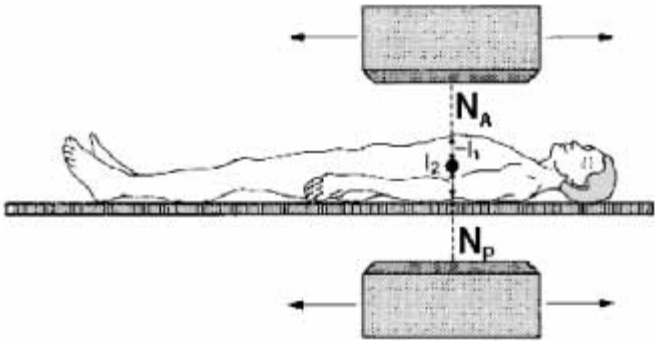

Fig. 1. Conjugate whole-body imaging with a dual-headed gamma-camera system. The counts measured from anterior (N_A) and posterior (N_P) are pixelwise geometrically averaged so that the resulting value is independent of the depth of the activity source within the body.

Myers [4] showed that the quotient $(\mu d_i/2)/(\sinh(\mu d_i/2))$ involving the organ thickness d is close to one, so that an exact calculation of this term is not necessary. The attenuation correction factor $e^{(\mu/2)L}$ includes the unknown absorption coefficient μ and the externally measurable (but variable) body thickness L. Sometimes $e^{(\mu/2)L}$ is assumed to be constant so that the activity A_i becomes proportional to N_{GMi}. This assumption may be valid, if only not much activity is taken up by the extremities and by the lung and if the trunk is regarded as being constantly thick.

In an alternate approach, $e^{(\mu/2)L}$ can be determined by transmission scans. The transmission scan should be performed for every measurement. If it is only acquired once, exact repositioning of the patient for all subsequent scans is necessary. In order to simplify the procedure, relative attenuation factors might be determined in some subjects by transmission measurements using a flood source filled with the appropriate radionuclide. Specific correction factors can be obtained for head, neck, arms and legs as done by Krahwinkel *et al.* [5]. These authors corrected for the inhomogeneous thickness of the trunk by assuming its cross section to be elliptical. After calculation of the geometrically averaged count rate in each pixel, the multiplicative corrections are performed for the regions of trunk, arms, legs and thorax. This provides a corrected count rate N_{GMC} for each pixel of the patient's scan. This count rate is assumed to be proportional to the activity underlying the single pixels [5]. The activity A_{Organ} of a particular organ relative to the total body activity A_{Total} is given by:

$$A_{Organ} = A_{Total} \frac{\sum_{Organ} N_{GMC}}{\sum_{Total} N_{GMC}} \tag{3}$$

$\sum_{Organ} N_{GMC}$: Sum of corrected pixel count rates over the organ of interest

$\sum_{Total} N_{GMC}$: Sum of corrected pixel count rates over total body

At our centre this procedure was implemented in the study of the biodistribution of ^{201}Tl [5], ^{123}I-heptadecanoic acid [6] and ^{123}I-α-methyltyrosine [1].

In the case of ^{201}Tl, organs overlapping in the conjugate views had to be taken into account: liver and right kidney or stomach and left kidney, respectively. For this purpose an additional correction procedure was developed which utilised the low photon energy of ^{201}Tl [4]. The method was vali-

Table 2. Biodistribution of ^{201}Tl (taken from [5]).

Organ	Time after Injection (hours)					
	2	24	48	120	168	216
Whole-body	100	95.1±2.7	90.5±3.0	75.3±5.7	68.7±6.5	63.3±7.4
Brain	1.5±0.3	1.7±0.3	1.8±0.3	2.1±0.2	1.9±0.3	1.8±0.2
Facial part	3.1±0.5	3.2±0.4	3.2±0.5	2.9±0.4	2.7±0.5	2.3±0.3
Neck	1.2±0.2	1.2±0.1	1.1±0.1	0.9±0.1	0.8±0.2	0.7±0.2
Thyroid	0.5±0.1	0.5±0.1	0.5±0.1	0.4±0.1	0.3±0.1	0.3±0.1
Heart	3.9±0.9	2.9±0.6	2.6±0.4	2.1±0.3	1.8±0.3	1.5±0.4
Thorax (no heart)	6.2±0.6	6.1±0.5	5.8±0.6	4.7±0.6	4.1±0.6	3.5±0.7
Liver	5.1±0.7	4.1±0.5	3.8±0.3	3.1±0.4	2.7±0.3	2.4±0.3
Stomach	3.2±0.5	2.5±0.5	2.2±0.4	1.8±0.3	1.6±0.3	1.5±0.3
Spleen	1.0±0.2	0.9±0.1	0.8±0.1	0.7±0.1	0.6±0.1	0.6±0.1
Intestine	20.1±2.2	20.7±1.7	19.7±1.7	15.2±2.0	13.0±2.0	10.7±2.4
Kidneys	5.6±1.4	4.6±0.8	4.2±0.6	3.4±0.6	3.0±0.4	2.5±0.5
Arms	5.1±0.9	6.7±1.0	6.7±0.9	5.8±0.9	5.3±0.8	5.0±0.9
Legs	26.2±4.0	23.0±2.2	21.0±2.3	17.3±2.0	15.9±2.0	15.4±1.6
Thigh	18.2±2.4	15.0±1.5	13.2±1.6	10.5±1.4	9.5±1.3	9.3±0.9
Lower leg, foot	7.7±1.8	8.1±1.2	7.8±0.9	6.8±0.8	6.4±0.7	6.0±0.7
Femoral muscles	16.3±2.2	13.1±1.5	11.4±1.5	9.1±1.2	8.1±1.2	8.0±0.8
Tibia muscles	5.9±1.4	5.7±0.9	5.5±0.7	4.6±0.6	4.3±0.5	4.2±0.5
Testis (n=14)	0.4±0.1	0.3±0.1	0.3±0.1	0.3±0.1	0.3±0.1	0.3±0.1

Mean and standard deviation of the whole-body and relative organ activities in 15 patients (Units are % injected activity, decay corrected)

dated by three tests with an anthromorphologic whole-body Alderson phantom applying different distributions of activity. In these tests, the errors were less than 14%, so the biodistribution data for ^{201}Tl shown in Table 2 and Fig. 2 can be considered reasonably accurate.

Whole-body scans have to be done several times after injection. The definite times must be chosen in respect to the physical and biological decay of the radiopharmaceutical [7]. In the case of a very slow biological removal the measurements should cover a period of up to 3 or 4 physical half-lives. Afterwards, the count rates become so low that the statistical errors become considerable. If the measurements cannot be extended so long, the measured data have to be extrapolated until the physical decay of the radionuclide – practically five half-lives as demonstrated below (Fig. 4).

Generally, it is possible to combine the whole-body measurements with the diagnostic investigation, which is commonly done shortly after the injection. After the diagnostic procedure whole-body scans can be done on the same day and if necessary during the following days. No additional radiation dose is received by the subject due to these whole-body measurements; a relatively small dose results from performance of a transmission scan.

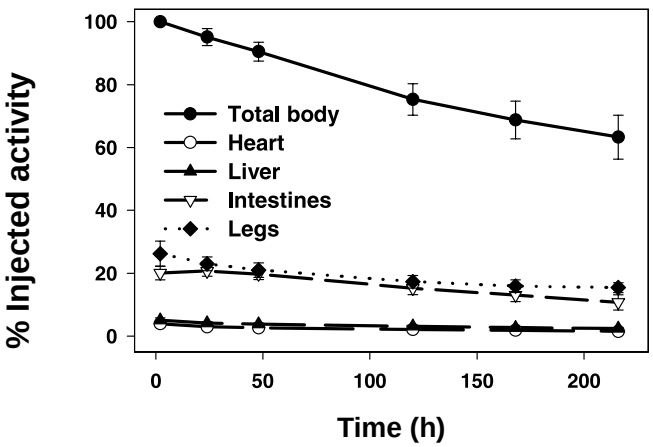

Fig. 2. Time activity curves after the injection of ^{201}Tl. The measured decay-corrected radioactivity data are related to the amount of injected radioactivity (= 100%).

Biodistribution measurement of positron emitters

One of the main characteristics of PET is its ability to quantify radioactivity within the body in absolute terms. Therefore, diagnostic studies may supply biodistribution data as well. This is especially true for oncological whole-body studies such as those done with ^{18}F-fluorodeoxyglucose (FDG). These studies are, however, only quantitative if they are corrected for attenuation with the help of additional transmission scans. In order to know the biodistribution at more than one time, it is necessary to repeat the whole-body scans after an appropriate period. In the case of ^{18}F-labelled radiopharmaceuticals it may be sufficient to do 3 scans, e.g. at 30–60 minutes, at 4 hours and at 6 hours after injection, in this way covering three half-lives of the tracer. Uptake data are obtained by defining regions of interest over the single organs in all these transversal images in which the organ is visible, so that the total activity within the organ as well as the volume of the organ are obtained. The PET measurement must be accompanied by measurements of excretion. In most cases, it is sufficient to just measure the activity in urine, as fecal elimination continues for a long time, over which the radionuclide typically has decayed to negligible levels. If the half-life of a positron emitter is longer than that of ^{18}F, as in the case of ^{86}Y ($T_{1/2} = 14.7$ h), the whole-body measurement must be repeated on a second or third day and the necessity of measuring the feces must be checked.

If radiopharmaceuticals are labelled with short-lived radionuclides such as ^{11}C or ^{15}O, whole-body measurements are no longer possible. Whole-body measurements may also not be compatible with the diagnostic investigation of an ^{18}F-labelled radiopharmaceutical, if a long static or dynamic

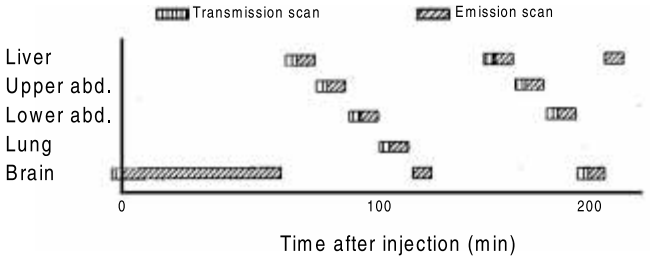

Fig. 3. Schedule of transmission and emission scans over different organs for the measurement of the biodistribution of the dopamine2 receptor ligand ^{18}F-fluoro-ethyl-spiperone.

acquisition is needed in respect to one single organ. Then, it may be sufficient to interrupt the diagnostic measurements for 5 or 10 min and to do a quick scan over other organs with possibly relevant uptake. By looking at one organ in some patients and at other organs in different patients intersubject uptake data are collected. An example of an acquisition scheme which was performed for the ^{18}F-labelled D2-receptor ligand [^{18}F]-fluoro-ethyl-spiperone is shown in Fig. 3 [8].

Even in the case of the ultra-short lived radionuclide ^{15}O ($T_{1/2} = 2.03$ min) it was possible to obtain all biodistribution data relevant to dosimetry of ^{15}O-butanol [9]. In this case it was not possible to combine all necessary studies with the diagnostic procedure so that some studies had to be performed just for the measurement of the biodistribution. However, only a small part of the activity used for the diagnostic procedure needed to be injected, so that the radiation dose to those subjects volunteering for the biodistribution measurements was kept very low.

In those cases where it is difficult to collect the necessary biodistribution data – maybe because of the short half-life of the tracer – model based analyses of biodistribution have been suggested. Especially in the case of ^{15}O-labelled water, a number of models have been reported leading to quite different radiation doses [10–13].

The unique ability of PET to quantify radioactivity can also be exploited for the measurement of non-positron emitting radionuclides. Many radionuclides used for diagnosis and therapy in nuclear medicine have positron emitting analogues so that PET can help to get quantitative biodistribution data for those radiopharmaceuticals which are difficult to evaluate otherwise. This approach was first suggested at Jülich for purely β^--emitting therapeutic radioisotopes [14]. Table 3 gives a list of radionuclides and their positron emitting analogues. The only externally measurable radiation in case of pure β^--emitters is bremsstrahlung yielding crude image information which is difficult to quantify. The positron emitter ^{86}Y was used to estimate the radiation dose caused by some radiotherapeuticals labelled with β^--emitting ^{90}Y [14]. ^{86}Y/^{90}Y labelled citrate and EDTMP were studied in patients suffering from prostate cancer to estimate the radiation dose caused by the ^{90}Y-compounds to normal tissue but also to metastases [15]. The biodistribution of ^{86}Y/^{90}Y-DOTA-octreotide was investigated in baboons to prepare the clinical trial phase II [16]. There are other β^--emitters used for radiotherapy which emit γ-radiation as well. Here conjugate whole-body imaging with whole-body gamma cameras can and has been applied as described above. On the other hand, the additional use of positron emitting radioisotopes can improve the quantitative accuracy of those whole-body measurements. For example, ^{124}I might be useful to calibrate analyses done with whole-body single photon imaging or even SPECT studies [17].

Table 3. Beta-emitters and their positron-emitting analogues.

β^--emitter		β^+-emitting analogue		
	Half-life		Half-life	β^+-abundance
^{89}Sr	50.4 d	^{83}Sr	1.35 d	24%
^{90}Y	3.19 d	^{86}Y	14.7 h	33%
^{153}Sm	1.95 d	^{142}Sm	72 min	5.7%
^{131}I	8.02 d	^{124}I	4.18 d	63%

Calculation of absorbed dose

Knowing the biodistribution of a radiopharmaceutical, i.e. its distribution and biokinetics within the body, the estimation of the radiation dose consists of knowing the energy emitted along with the radiation and of determining that part of this energy which is absorbed in the various tissues of the body [18, 19]. Rarely does activity become taken up by an organ and remain there with no biological removal. Even in these cases, the activity diminishes with time, due to physical decay of the radionuclide. In order to calculate the radiation dose to the organ of uptake and other surrounding tissues, one must count all of the decays of the nuclide over time, from the moment of uptake until the final disappearance of the nuclide, due to physical decay and/or biological removal. The integral of the radioactivity $A(t)$ over time represents all of the radioactive events that occurred within the source organ:

$$\tilde{A} = \int_0^\infty A(t)\,\mathrm{d}\,t\,. \tag{4}$$

The integral of radioactivity over time starting from the injection up to the decay of the activity is called cumulated activity $\tilde{A}$. The term decay is not only related to the physical but also to the biological decay, i.e. the total elimination of activity. To calculate the cumulated activity one has to know the actual activity within a source organ as a function of time. Here the time-activity curve should not be decay-corrected. If, however, the cumulated activity has been determined using a decay-corrected time-activity curve the radioactive decay can be taken into account by the following equation

$$\tilde{A} = \tilde{A}^{\text{decay-corrected}}\, T_{1/2}/\ln(2) = \tilde{A}^{\text{decay-corrected}}\, 1.443 T_{1/2}\,, \tag{5}$$

where $T_{1/2}$ is the half-life, which relates to λ^{phys}, the physical decay constant of the radionuclide, as follows

$$1/\lambda^{\text{phys}} = 1.443 T_{1/2}\,. \tag{6}$$

Often, the cumulated activity is related to the total administered activity A_o. In this case, the unit of radioactivity is

cancelled out leaving an expression with the unit time. Although not being a truly physical time, this entity is called residence time τ.

$$\tau = \tilde{A}/A_o\,. \tag{7}$$

If A_i is a part of the total injected activity A_o and initially taken up in organ i, from which it is released according to a monoexponential outwash with a biological time constant λ^{biol}, the residence time τ can be calculated as follows

$$\tau = 1/(\lambda^{\text{phys}} + \lambda^{\text{biol}})(A_i/A_o) = 1.443 T_{1/2}^{\text{eff}}(A_i/A_o) \tag{8}$$

$T_{1/2}^{\text{eff}}$ is the effective half-life indicating after which time half of a radiopharmaceutical has left an organ by both physical decay and biological removal.

Although the upper integration limit of (4) is infinity, activity values may be available only over a relatively short period. Therefore, $A(t)$ has to be extrapolated beyond this period. For this purpose the measured data may be fitted using an appropriate function which is then extrapolated out to several half-lives of the radionuclide. Fig. 4 shows fitted curves found for a fictitious data set, of which the last data point exhibits a 10% error, without and with decay correction. Curves corrected for decay showed a great uncertainty due to this error, while curves including radioactive decay all decrease rapidly, so that after five half-lives the residual activity amounts only to 3% of the original activity at the time of injection. The dominant role of the radioactive decay makes an inaccuracy in the fitting and extrapolation process less important.

Rarely do the measured values in all organs comprise 100% of the injected activity. Usually the most important organs account for some percent of the total, and the remainder is distributed more or less uniformly throughout all other tissues. In this case, the MIRD formalism introduces the concept of the remainder of the body. The remainder of the body is the difference between the total administered dose and the sum of all specifically known activities. The remainder (activity) of the body is again a function of time and its integral over time provides the cumulated activity or residence time, respectively, of the remainder of the body. In most applications, elimination from the body is primarily by urinary excretion and secondarily, if at all, via the fecal pathway. A proper balance of the biodistribution has to include these pathways. For this purpose reliable excreta measurements must be made. From this data the total activity remaining in the body can be calculated.

When the cumulated activities $\tilde{A}_j$ of all organs with relevant uptake and of the remainder of the body have been determined, the dose absorbed D_i in these organs and in other organs (targets) receiving radiation from the source organs j can be calculated:

$$D_i = S_{ij}\tilde{A}_j \tag{9}$$

The so called S-factor represents the radiation dose received in a target organ i per unit activity located in a source organ j [18]. The target and source organ may be identical. The radiation dose to an organ is the sum of all doses caused by the activity in the organ itself and from all surrounding tissues:

$$D_i = \sum_j S_{ij}\tilde{A}_j \tag{10}$$

The S-factor itself is a product of several entities according to the following equation:

$$S_{ij} = nE\,\phi_{ij}/m_i \tag{11}$$

where nE is the mean energy emitted per nuclear decay, ϕ_{ij} is the absorbed fraction (i.e. that part of the radiation energy emitted from source j which is absorbed in target i), and m_i is the mass of the target. The absorbed fraction is dependent on the shape of the source and target organs and on

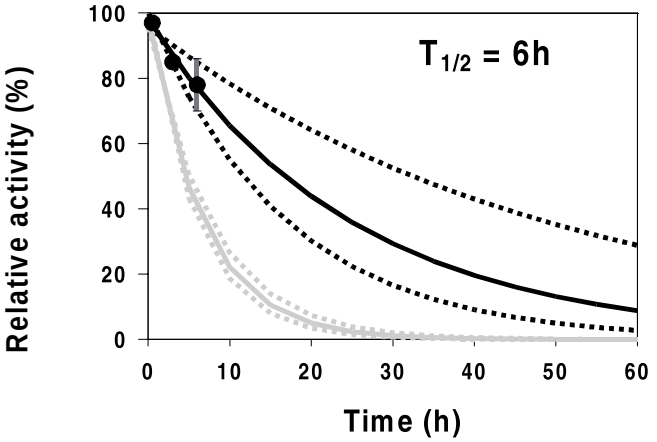

Fig. 4. To calculate the cumulated activity the three data points have to be extrapolated. Large differences result in the extrapolated curves (black), due to the uncertainties of the last data point. This variance and in this way the integral under the curves (cumulated activity) is considerably decreased when the decay is taken into account (grey curves). The decay corrected curves are very close to zero at five physical half-lives of the radionuclide.

Table 4. Radiation dose from intravenous administration of ^{201}Tl for heart planar scintigraphy or SPECT.

Target organ $n = 15$	Radiation Dose mGy/MBq	mrad/mCi
Adrenals	0.011 ± 0.002	0.039 ± 0.007
Bladder wall	0.012 ± 0.002	0.044 ± 0.009
Bone	0.013 ± 0.003	0.047 ± 0.010
Heart	0.009 ± 0.001	0.033 ± 0.005
Small intestines	0.017 ± 0.003	0.061 ± 0.010
Upper large int.	0.070 ± 0.020	0.260 ± 0.075
Lower large int.	0.145 ± 0.044	0.537 ± 0.163
Kidney	0.064 ± 0.011	0.236 ± 0.040
Liver	0.015 ± 0.002	0.054 ± 0.008
Lungs	0.009 ± 0.002	0.034 ± 0.007
Red marrow	0.017 ± 0.003	0.063 ± 0.013
Muscle	0.009 ± 0.002	0.034 ± 0.007
Pancreas	0.013 ± 0.003	0.049 ± 0.010
Skin	0.007 ± 0.001	0.025 ± 0.005
Spleen	0.027 ± 0.007	0.099 ± 0.027
Stomach wall	0.028 ± 0.007	0.105 ± 0.026
Testes (n=14)	0.091 ± 0.058	0.336 ± 0.214
Thyroid	0.092 ± 0.023	0.341 ± 0.087
Uterus ($n = 1$)	0.015	0.050
Effective dose equivalent	0.096 ± 0.047 mSv/MBq	0.356 ± 0.176 mrem/mCi

These results are based on the biodistribution data shown in Fig. 2 and Table 2

Table 5. ICRP 26 [23]: Effective dose equivalent: $H_E = \sum w_i D_i$.

Tissue	w_i
Gonads	0.25
Breast	0.15
Red marrow	0.12
Lung	0.12
Thyroid	0.03
Bone surfaces	0.03
Remainder	0.30

Remainder: Assign a weight of 0.06 to each 5 organs of the remainder with the highest D_i.

Table 6. ICRP 60 [34]: Effective dose: $H_E = \sum w_i D_i$.

Tissue	w_i
Gonads	0.20
Colon	0.12
Red morrow	0.12
Lung	0.12
Stomach	0.12
Bladder	0.05
Breast	0.05
Liver	0.05
Oesophagus	0.05
Thyroid	0.05
Skin	0.01
Bone surfaces	0.01
Remainder	0.05

Remainder: Assign a weight of 0.05 to the mean dose of adrenals, brain, upper large intestine, small intestine, kidney, muscle, pancreas, spleen, thymus, and uterus.

the distance between them, as well as on the structures of other tissues situated between the source and target. For γ-radiation ϕ is less than one, whereas for β-radiation, which is assumed not to escape the source, ϕ is equal to one [19]. For diagnostic purposes, it is not feasible to use *S*-factors for an individual patient. Instead *S*-factors are based on the geometrical relationship which have been defined for a human standard phantom [18, 20]. In order to estimate the dose caused by an individual radionuclide therapy, the target mass and the source-target relationship should be derived from the patient-specific geometry obtained from computed tomography or magnet resonance imaging [21].

Knowing the cumulated activities of all single source organs and of the remainder of the body the doses absorbed by the target organs (including the total body) can be calculated, resulting in a table such as shown in Table 4.

Some years ago, Stabin [22] has published a very valuable program called MIRDOSE (present version MIRDOSE3) which requires the residence times as input data, contains S-factors of numerous radionuclides, and yields a list of radiation doses to single organs as well as the whole-body dose according to ICRP 26 [23] and ICRP 60 [24], respectively (see below). The MIRDOSE3 program also includes the specific considerations necessary for calculating the radiation dose of the urinary bladder and the gastro-intestinal tract. The estimation of the bladder dose applies the sugges-

Table 7. Some commonly used SPECT and PET radiopharmaceuticals and the resulting effective doses.

Radiopharmaceutical	Function	Effective dose equivalent (mSv/MBq)	Effective Dose (mSv/MBq)	Reference
Used for SPECT				
^{99m}Tc-HMPAO	Brain blood flow	0.012		[27]
^{99m}Tc-ECD	Brain blood flow	0.008		[28]
^{99m}Tc-sestamibi	Heart blood flow	0.004		[29]
^{99m}Tc-tetrofosmin	Heart blood flow		0.0089	[30]
^{99m}Tc-DMSA	Renal function	0.005		[31]
^{99m}Tc-TRODAT	Dopamin-transporter	0.015	0.012	[32]
^{111}In-DTPA-D-Phe-1-octreotide	Somatostatin receptor ligand	0.080		[33]
^{111}In-pentetreotide	Somatostatin receptor ligand	0.100	0.073	[34]
^{123}I-IMP	Brain blood flow	0.024		[35]
^{123}I-IBZM	Dopamin2-receptor-ligand	0.034		[36]
^{123}I-iomazenil	Benzodiazepine receptor ligand	0.033		[37]
^{123}I-epidepride	Dopamin2-receptor-ligand	0.035		[38]
^{123}I-ß-CIT	Dopamin-transporter	0.024		[39]
^{131}I-IgM	Immunoscintigraphy	0.120		[40]
^{191m}Ir	Blood flow	0.004		[41]
^{201}Tl	Heart blood flow	0.096		[4]
Used for PET				
^{11}C-N-methylspiperone	Dopamin2-receptor-ligand	0.007		[42]
^{11}C-raclopride	Dopamin2-receptor-ligand	0.003		[43]
^{11}C-iomazenil	Benzodiazepine receptor ligand	0.015		[44]
^{11}C-glucose	Glucose metabolism	0.004 m/0.005 f		[45]
^{11}C-methionine	Amino acid tracer		0.0052	[46]
^{11}C-acetate	Heart oxygen metabolism	0.004		[42]
^{13}N-ammonia	Heart blood flow	0.003		[42]
^{15}O-water	Blood flow	0.001	0.001150	[12]
^{18}F-FDG	Glucose metabolism	0.019		[42]
^{18}F-L-dopa	Dopamin-pool	0.018		[47]
^{18}F-fluoromisonidazole	Hypoxia marker		0.013m/0.014f	[48]

tion of Cloutier and coworkers [25], for which the voiding interval is an important variable.

To our knowledge, there has been no unified tool which offers the fitting and extrapolation of the measured time-activity data, the calculation of the cumulated activities as well as the calculation of the radiation doses for the single organs and the total body. Therefore, our group developed an Excel program which combines all these steps so that the whole procedure is considerably facilitated [26].

In order to characterise the amount of radiation dose and in this way also the risk caused by a specific nuclear medicine procedure, previous papers reported the highest of all single organ doses and the dose to the total body. The organ with the highest dose was called critical organ.

This approach, however, does not take into account that some organs are more radiation-sensitive than others. Therefore, ICRP 26 has also considered the radiobiological sensitivity of different organs in respect to the ionising radiation. For this purpose the radiation dose caused to the whole-body dose is described by the so-called effective dose equivalent (H_E), which is a weighed sum of the radiation doses primarily to those organs which are regarded as radiation-sensitive.

$$H_E = \sum w_i D_i \tag{12}$$

This formula is valid for X-rays, γ- and β-radiation. The suggestions of ICRP 26 [23] have been revised by ICRP 60 [24] which replaced the term effective dose equivalent by the effective dose and modified the weighting factors w_i. Tables 5 and 6 display the weighting factors as suggested by ICRP 26 and ICRP 60. Although ICRP 60 is the up-to-date international recommendation, national rules and dose limits are partly still based on ICRP 26.

Radiation doses in SPECT and PET studies

Table 7 presents the data of the effective dose equivalent and effective dose, respectively, caused by commonly used SPECT and PET radiopharmaceuticals.

In order to compare these values they must be multiplied with the amount of radioactivity which has to be administered to assure a satisfactory image quality needed for diagnosis or scientific evaluation. In general, the dose to a patient must be judged in relation to the expected benefit by the SPECT or PET examination, whereas the dose to volunteers is limited by national regulation.

Concluding remark

This paper presents a review of in vivo methods to obtain the biodistribution of radiopharmaceuticals used with SPECT and PET as well as the description of dosimetric calculations. The interested reader will find more detailed information about these issues in some recent articles and MIRD reports [7, 49–51].

Acknowledgment. The author gratefully appreciates the detailed comments and suggestions given by the referee and thanks for the secretarial help of Mrs. M. Bunn.

References

1. Schmidt, D., Langen, K.-J., Herzog, H., Wirths, J., Holschbach, M., Kiwit, J. C., Ziemons, K., Coenen, H. H., Müller-Gärtner, H.-W.: Whole-body kinetics and dosimetry of L-3–123I-iodo-alpha-methyltyrosine. Eur. J. Nucl. Med. **24**, 1162–1166 (1997).
2. Budinger, T. F.: Quantitative nuclear medicine imaging: application of computers to the gamma camera and whole-body scanner. In: *Progress in Atomic Medicine*. Vol.4., Recent Advances in Nuclear Medicine, (J.H. Lawrence, ed.). Grune & Stratton, New York, p. 41–130 (1974).
3. Sorensen, J. A.: Quantitative measurement of radioactivity in vivo by whole-body counting. In: *Instrumentation in Nuclear Medicine* (G.J. Hine, et al. and J.A. Sorenson. J. A., eds.). Vol. 2, New York, Academic Press, p. 311–347 (1974).
4. Myers, M. J., Lavender, J. P., de Oliveira, J. B., Maseri, A.: A simplified method of quantitating organ uptake using a gamma camera. British J. Radiol. **54**, 1062–1067 (1981).
5. Krahwinkel, W., Herzog, H., Feinendegen, L. E.: Pharmacokinetics of Thallium-201 in normal individuals after routine myocardial scintigraphy. J. Nucl. Med. **29**, 1582–1586 (1988).
6. Abels, P. D. R.: Quantifizierung der Radionuklidverteilung der Organe im Ganzkörper nach i.v.-Injektion von omega-J-123-Heptadekansäure. MD-Thesis at the Medical Faculty of Heinrich-Heine University Düsseldorf (1988).
7. Siegel, J. A., Thomas, S. R., Stubbs, J. B., *et al.*: MIRD pamphlet no. 16: Techniques for quantitative radiopharmaceutical biodistribution data acquisition and analysis for use in human radiation dose estimates. J. Nucl. Med. **40**, 37S–61S (1999).
8. Herzog, H., Coenen, H. H., Kuwert, T., Langen, K.-J., Feinendegen, L. E.: Quantitation of the whole-body distribution of PET radiopharmaceuticals: Applied to 3-N-([18F]fluoroethyl)spiperone. Eur. J. Nucl. Med. **16**, 77–83 (1990).
9. Herzog, H., Seitz, R. J., Tellmann, L., Schlaug, G., Kleinschmidt, A., Nebeling, B., Stöcklin, G., Müller-Gärtner, H. W.: Pharmacokinetics and radiation dose of oxygen-15 labelled butanol in rCBF studies in humans. Eur. J. Nucl. Med. **21**, 138–143 (1994).
10. Jones, S.C., Greenberg, J.H., Dann, R., Robinson, G.D. Jr., Kushner, M., Alavi, A., Reivich, M.: Cerebral blood flow with the continuous infusion of oxygen-15-labeled water. J. Cereb. Blood Flow Metab. **5**, 566–755 (1985).
11. Smith, T., Tong, C., Lammertsma, A.A., Butler, K.R., Schnorr, L., Watson, J.D., Ramsay, S., Clark, J.C., Jones, T.: Dosimetry of intravenously administered oxygen-15 labelled water in man: a model based on experimental human data from 21 subjects. Eur. J. Nucl. Med. **21**, 1126–1134 (1994).
12. Brihaye, C., Depresseux, J. C., Comar, D.: Radiation dosimetry for bolus administration of oxygen-15-water. J. Nucl. Med. **36**, 651–656 (1995).
13. Narayana, S., Hichwa, R.D., Ponto, L.L., Hurtig, R.R., Watkins, G.L.: Construction of a whole body blood flow model for use in positron emission tomography imaging with [15O]water. J. Pharmacokinet. Biopharm. **25**, 539–568 (1997).
14. Herzog, H., Rösch, F., Stöcklin, G., Lueders, C., Qaim, S. M., Feinendegen, L. E.: Measurement of pharmacokinetics of Yttrium-86 radiopharmaceuticals with PET and radiation dose calculation of analogous Yttrium-90 radiotherapeutics. J. Nucl. Med. **34**, 2222–2226 (1993).
15. Rösch, F., Herzog, H., Plag, C., Neumaier, B., Braun, U., Müller-Gärtner, H.-W., Stöcklin, G.: Radiation doses of yttrium-90 citrate and yttrium-90 EDTMP as determined via analogous yttrium-86 complexes and positron emission tomography. Eur. J. Nucl. Med. **23**, 958–966 (1996).
16. Rösch, F., Herzog, H., Stolz, B., Brockmann, J., Köhle, M., Mühlensiepen, H., Marbach, P., Müller-Gärtner H.-W.: Uptake kinetics of the somatostatin receptor ligand [86Y]DOTA-DPhe1-Tyr3-octreotide ([86Y]SMT487) using positron-emission-tomography in non-human primates and calculation of radiation doses of the 90Y-labelled analogue. Eur. J. Nucl. Med. **26**, 358–366 (1999).
17. Langen, K.-J., Coenen, H. H., Roosen, N., Kling, P., Muzik, O., Herzog, H., Kuwert, T., Stöcklin, G., Feinendegen, L. E.: SPECT studies of brain tumors with L-[123I]iodo-methyl-tyrosine

(123IMT): First clinical results and comparison with PET and 124IMT. J. Nucl. Med. **31**, 281–286 (1990).
18. Snyder, W. S., Ford, M. R., Warner, G. G., *et al.*: "S," Absorbed dose per unit cumulated activity for selected radionuclides and organs. MIRD Pamphlet No. 11, New York, The Society of Nuclear Medicine (1975).
19. Loevinger, R., Budinger, T. F., Watson, E. E.: MIRD-Primer for absorbed dose calculations. New York, The Society of Nuclear Medicine (1988).
20. ICRP-23: Report of the task group of reference man. Recommendations of the International Commission on Radiological Protection, ICRP-Publication 23, Pergamon Press (1975).
21. Kolbert, K.S., Sgouros, G., Scott, A.M., Bronstein, J.E., Malane, R.A., Zhang, J., Kalaigian, H., McNamara, S., Schwartz, L., Larson. S.M. Implementation and evaluation of patient-specific three-dimensional internal dosimetry. J. Nucl. Med. **38**, 301–308 (1997).
22. Stabin, M. G.: MIRDOSE: Personal computer software for internal dose assessment in nuclear medicine. J. Nucl. Med. **37**, 538–546 (1996).
23. ICRP-26, Radiation Protection. Recommendations of the International Commission on Radiological Protection, ICRP-Publication 26, Pergamon Press (1977).
24. ICRP-60, 1990 Recommendations of the International Commission on Radiological Protection, ICRP-Publication 60, Pergamon Press (1991).
25. Cloutier, R. J., Smith, S. A., Watson, E. E., *et al.*: Dose to the fetus from radionuclides in the bladder. Health Physics **25**, 147–161 (1973).
26. Herzog, H., Zilken, H., Niederbremer, A., Friedrich, W., Müller-Gärtner, H.-W.: Calculation of Residence Times and Radiation Doses Using the Standard PC-Software Excel. Eur. J. Nucl. Med. **24**, 1514–1522 (1997).
27. Huda, W., Sandison, G. A.: The use of the effective dose equivalent, HE, for 99mTc labelled radiopharmaceuticals. Eur. J. Nucl. Med. **15**, 174–179 (1989).
28. Holman, B. L., Hellman, R. S., Goldsmith, S. J., Mena, I. G., Leveille, J., Gherardi, P. G., Moretti, J. L., Bischof-Delaloye, A., Hill, T. C., Rigo, P. M., *et al.*: Biodistribution, dosimetry, and clinical evaluation of technetium-99m ethylcysteinate dimer in normal subjects and in patients with chronic cerebral infarction. J. Nucl. Med. **30**, 1018–1024 (1989).
29. Wackers, F. J., Berman, D. S., Maddahi, J., Watson, D. D., Beller, G. A., Strauss, H. W., Boucher, C. A., Picard, M., Holman, B. L., Fridrich, R., et al.: Technetium-99m hexakis 2-methoxyisobutyl isonitrile: human biodistribution, dosimetry, safety, and preliminary comparison to thallium-201 for myocardial perfusion imaging. J. Nucl. Med. **30**, 301–311 (1989).
30. Higley, B., Smith, F. W., Smith, T., Gemmell, H. G., Das Gupta, P., Gvozdanovic, D. V., Graham, D., Hinge, D., Davidson, J., Lahiri, A.: Technetium-99m-1,2-bis[bis(2-ethoxyethyl) phosphino]ethane: human biodistribution, dosimetry and safety of a new myocardial perfusion imaging agent. J. Nucl. Med. **34**, 30–38 (1993).
31. Watkinson, J. C., Allen, S., Lazarus, C. R., Sinclair, J., Blake, G. M., Clarke, S. E.: Pharmacokinetics, biodistribution and dosimetry of 99Tcm(V)DMSA in humans with squamous cell carcinoma. Nucl. Med. Commun. **11**, 343–359 (1990).
32. Mozley, P. D., Stubbs, J. B., Plossl, K., Dresel, S. H., Barraclough, E. D., Alavi, A., Araujo, L. I., Kung, H. F.: Biodistribution and dosimetry of TRODAT-1: a technetium-99m tropane for imaging dopamine transporters. J. Nucl. Med. **39**, 2069–2076 (1998).
33. Krenning, E. P., Bakker, W. H., Kooij, P. P., Breeman, W. A., Oei, H. Y., de Jong, M., Reubi, J. C., Visser, T. J., Bruns, C., Kwekkeboom, D. J., *et al.*: Somatostatin receptor scintigraphy with indium-111-DTPA-D-Phe-1-octreotide in man: metabolism, dosimetry and comparison with iodine-123-Tyr-3-octreotide. J. Nucl. Med. **33**, 652–658 (1992).
34. Stabin, M. G., Kooij, P. P., Bakker, W. H., Inoue, T., Endo, K., Coveney, J., de Jong, R., Minegishi, A.: Radiation dosimetry for indium-111-pentetreotide. J. Nucl. Med. **38**, 1919–1922 (1997).
35. Holman, B. L., Zimmerman, R. E., Schapiro, J. R., Kaplan, M. L., Jones, A. G., Hill, T. C.: Biodistribution and dosimetry of N-isopropyl-p-[123I]iodoamphetamine in the primate. J. Nucl. Med. **24**, 922–931 (1983).
36. Verhoeff, N. P., Sokole, E. B., Stabin, M., Hengst, D., Kung, H. F., Van Royen, E. A., Janssen, A. G.: Dosimetry of iodine-123 iodobenzamide in healthy volunteers. Eur. J. Nucl. Med. **20**, 747–752 (1993).
37. Verhoeff, N. P., Busemann Sokole, E., Hengst, D., Stubbs, J. B., van Royen, E. A.: Dosimetry of iodine-123 iomazenil in humans. Eur. J. Nucl. Med. **20**, 580–584 (1993).
38. Kuikka, J. T., Akerman, K. K., Hiltunen, J., Bergstrom, K. A., Rasanen, P., Vanninen, E., Halldin, C., Tiihonen, J.: Striatal and extrastriatal imaging of dopamine D2 receptors in the living human brain with [123I]epidepride single-photon emission tomography. Eur. J. Nucl. Med. **24**, 483–487 (1997).
39. Booij, J., Busemann Sokole, E., Stabin, M. G., Janssen, A. G. M., de Bruin, K., van Royen, E. A.: Human biodistribution and dosimetry of [123I]FP-CIT: a potent radioligand for imaging of dopamine transporters. Eur. J. Nucl. Med. **25**, 24–30 (1998).
40. Roos, J. C., Plaizier, M. A., van Lingen, A., Haisma, H. J., den Hollander, W., Martens, H. J., Nauta, J. J., Dejager, R. L., Teule, G. J., Boven, E.: Distribution and kinetics of 131I-labelled human IgM monoclonal antibody 16.88 in patients with advanced colorectal cancer. In Vivo **7**, 503–509 (1993).
41. Treves, S. T., Fung, L., Packard, A. B.: Rapid renal single-photon emission tomography by continuous infusion of iridium-191m. Eur. J. Nucl. Med. **26**, 489–493 (1999).
42. Huda, W., Sandison, G. A.: Estimates of the effective dose equivalent, HE, in positron emission tomography studies. Eur. J. Nucl. Med. **17**, 116–220 (1990).
43. Mazière, B., Coenen, H. H., Halldin, C., Nagren, K., Pike, V. W.: PET radioligands for dopamine receptors and re-uptake sites: chemistry and biochemistry. Nucl. Med. Biol. **19**, 497–512 (1992).
44. Baldwin, R. M., Horti, A. G., Bremner, J. D., Stratton, M. D., Dannals, R. F., Ravert, H. T., Zea-Ponce, Y., Ng, C. K., Dey, H. M., Soufer, R., *et al.*: Synthesis and PET imaging of the benzodiazepine receptor tracer [N-methyl-11C]iomazenil. Nucl. Med. Biol. **22**, 659–665 (1995).
45. Graham, M. M., Peterson, L. M., Muzi, M., Graham, B. B., Spence, A. M., Link, J. M., Krohn, K. A.: 1-[Carbon-11]-glucose radiation dosimetry and distribution in human imaging studies. J. Nucl. Med. **39**, 1805–1810 (1998).
46. Deloar, H.M., Fujiwara, T., Nakamura, T., Itoh, M., Imai, D., Miyake, M., Watanuki, S.: Estimation of internal absorbed dose of L-[methyl-11C]methionine using whole-body positron emission tomography. Eur. J. Nucl. Med. 1998 Jun; **25**(6) 629–633.
47. Harvey, J., Firnau, G., Garnett, E. S.: Estimation of the radiation dose in man due to 6-[18F]fluoro-L-Dopa. J. Nucl. Med. **26**, 931–935 (1985).
48. Graham, M. M., Peterson, L. M., Link, J. M., Evans, M. L., Rasey, J. S., Koh, W. J., Caldwell, J. H., Krohn, K. A.: Fluorine-18-fluoromisonidazole radiation dosimetry in imaging studies. J. Nucl. Med. **38**, 1631–1636 (1997).
49. Bolch, W. E., Bouchet, L. G., Robertson, J. S., *et al.*: MIRD pamphlet No. 17: the dosimetry of nonuniform activity distributions–radionuclide S values at the voxel level. Medical Internal Radiation Dose Committee. J .Nucl. Med. **40**, 11S–36S (1999).
50. Howell, R. W., Wessels, B. W., Loevinger, R., *et al.*: The MIRD perspective 1999. Medical Internal Radiation Dose Committee. J. Nucl. Med. **40**, 3S–10S (1999).
51. Stabin, M. G., Tagesson, M., Thomas, S. R., Ljungberg, M., Strand, S. E.: Radiation dosimetry in nuclear medicine. Appl. Radiat. Isot. **50**, 73–87 (1999).